

Organic solvent resistant membrane fabrication for waste water treatment process

S.Saravanan¹, G.Gnanapragasam¹, R.Gowrishankar² X.Joseph Vianny², Padmesh Medesety¹

¹Department of Chemical Engineering, V.S.B. Engineering College, Karur

²Department of Civil Engineering, V.S.B. Engineering College, Karur

Abstract:

Hollow fiber (HF) membranes have attracted rising attentions recently for organic solvent Nano filtration (OSN) applications. However, till now, hollow fiber OSN membranes are rarely reported, and most of them were prepared using expensive materials or special methods that are difficult to imply. In this study, a kind of HF OSN membrane with commonly used polyimide materials was prepared by a simple and feasible covalent-crosslinking strategy using polyethylenimine (PEI) of low molecular weight and 1,6-hexanediamine (HDA) to realize an integral crosslinking of the polyimide substrate and the skin layer, and using glutaraldehyde (GA) to further improve the dye rejection. The fabricated HF OSN membrane under optimal conditions has an ethanol permeance of $4.47 \text{ L m}^{-2} \text{ h}^{-1} \text{ MPa}^{-1}$, a Rhodamine B(479 Da) rejection of 96.5%, a mean pore size of $0.69 \pm 0.27 \text{ nm}$, as well as a good solvent stability according to the results of a 7-days stability tests in polar and non-polar solvents, implying promising OSN applications. The synergetic covalent-crosslinking strategy reported in this work could provide insightful guidance for the fabrication of high- performance HF OSN membrane.

Key word: Hollow Fiber, Nanofiltration. Membrane, organic solvent nanofiltration

1. Introduction:

Nanofiltration (NF) is a pressure-driven membrane process where low to moderately pressure (ranging from 5 to 60 bar) is applied. NF is used when low molecular solutes, such as inorganic salts or small organic molecules, have to be separated. Membranes applied in reverse osmosis (RO)/NF are mostly asymmetric with a dense, highly rejecting top layer (thickness $\sim 1 \text{ }\mu\text{m}$) supported by a more open,sublayer (thickness $\sim 50\text{--}500 \text{ }\mu\text{m}$). Both integral (when top layer and supporting layer are made of the same material) or composite (when top layer and supporting layer are made of different materials) membranes are used. The asymmetric structure of the NF membranes significantly decreases the pressure. required to accomplish filtration. NF has been widely applied to filtration of aqueous liquids. However, due to the lack of suitable membranes,

the application of NF in organic solvents is still limited. Recently, development of membranes suitable for organic solvent nanofiltration (OSN) has opened up a wide range of potential applications of NF for non-aqueous solutions.[1] OSN has a range of advantages over conventional separation processes, such as distillation or liquid chromatography.

OSN membranes having a good stability and performance in organic solvents can be used in pressure driven membrane separations to: a) purify organic solvents in order to reuse them. The separated solute is of insignificant interest, b) separate a molecule (or molecules) from a mixture, c) recover products, inhibitors or catalysts from reaction media, d) exchange solvents, e) combine a, b, c, or d.[2]

Some of examples of OSN applications are listed below: a) homogenous catalysts separation (separation of homogeneous transition metal complexes from the reaction products and solvents) b) edible oil processing (removal of phospholipids and pigments (“degumming”), extraction solvent recovery and deacidification of the oil)[3-6], c) processes in the petrochemical industry (dewaxing process, production of high quality aromatics, removal of Sulphur. d) processes in the pharmaceutical industry (concentration of antibiotics or pharmaceutical intermediates out of organic solvents, recovery of solvents used in preparative HPLC, solvent exchange in pharmaceutical synthesis chains).[7,8]. The MAX-DEWAX™ membrane process installed at Exxon Mobil’s Beaumont refinery is a first example of a large scale application of OSN.[9]. In OSN both polymeric and ceramic membranes stable in organic solvents can be used. As this work focuses on polymeric membranes only, these will be discussed in more detail. Polymeric membranes suitable for OSN are generally asymmetric membranes. Either integrally skinned (IS) or thin film composite (TFC) membranes are used. In IS type of membranes (which is a focus area of this work) both, the separation-determining, tight top layer, as well as a more open, porous bottom layer, are made in one step from the same material. On the other hand, in TFCs, a top layer and a supporting layer are made from different materials and are prepared in separate Steps.

2. Materials and methods

2.1 Chemicals

P84 polyimide was purchased from HP Polymer GmbH (Austria) and used without any pretreatment. Organic solvents (all obtained from Sigma-Aldrich, UK) used to prepare membranes were N,N-dimethylformamide (DMF), 1,4-dioxane, and isopropanol. The crosslinker

applied in this work was 1, 6-hexanediamine (HDA) purchased from Sigma Aldrich (UK). Titanium dioxide (nominal diameter = 5 nm) was obtained from American Elements (USA).

2.2 Membrane preparation

TiO₂ nanoparticles at loadings of 0, 1, 3, 5, and 10 wt. % based on the final dope composition were added to mixtures of DMF and 1,4-dioxane. PI was dissolved at room temperature in the above mixture to form polymer dope solutions of varying PI concentration. After complete polymer dissolution, dope solutions were placed in an ultrasonic bath for 5 h to prevent agglomeration of the nanoparticles, and then left overnight to disengage air bubbles before membrane casting. The dope solutions were then used to cast 300 µm thick viscous films on (i) a glass plate; or (ii) a polypropylene (PP) non-woven backing material (Viledon, Germany), using an adjustable casting knife (Elcometer 3700) on a bench casting machine (Braive Instruments). An evaporation period of 20 s was allowed before immersion into a water coagulation bath (20°C). The membranes were subsequently placed in an isopropanol solvent exchange bath to remove any residual water. The membranes to be crosslinked were transferred from isopropanol to the crosslinking solution (HDA in isopropanol). Following this, the membranes were rinsed with isopropanol to remove residual HDA. Both crosslinked and non-crosslinked membranes were finally subjected to the conditioning step in which membranes were kept overnight in a conditioning solution composed of polyethylene glycol 400/isopropanol (60/40 wt. %, respectively). Pieces of membranes to be used for wettability tests were not subjected to the conditioning step.

2.3 Membrane characterization

2.3.1 Viscosity test

Viscosities of dope solutions with varying concentrations of TiO₂ nanoparticles were investigated using a Cannon Instrument Company (Model 2020) viscometer at 20°C, at varying rotational speeds of the LV2 spindle.

2.3.2 WAXS analysis

Wide angle X-ray scattering measurements for the PI/TiO₂ membranes without the backing material, and TiO₂ nanopowder were performed on PANalytical X'Pert Pro Multi Purpose Diffractometer with CuK α radiation (λ =1.5418 Å) at 40 kV and 40 mA.

2.3.3 Combustion test

A combustion test was performed in order to evaluate whether TiO₂ is retained in the membrane during the immersion precipitation process. A PI/TiO₂ membrane, without the backing material, was dried to a steady mass at 120°C to remove any residual liquids. This was followed by combustion in a Carbolite ELF furnace at 900°C until all polymer was burned off and a steady mass of TiO₂ was recorded.

2.3.4 Porosity test

Porosity tests were conducted to compare volume of the pores of PI and PI/TiO₂ membranes with no backing material. Measurements of the dimensions of square sections of the membrane were made to calculate volume of the section followed by drying until constant mass was obtained. Dry samples were then weighed. The volume of the PI and PI/TiO₂ mixture corresponding to the mass of the dry PI and PI/TiO₂ membranes was calculated using densities given by the manufacturer, i.e. 1.34 g cm⁻³ and 4.23 g cm⁻³ for P84 and TiO₂, respectively. The difference between the volume of the membrane samples and the volume of the corresponding amount of PI and the PI/TiO₂ mixture was calculated to yield the volume of the pores of the PI or PI/TiO₂ membranes. The percentage porosity the membranes (A) was calculated according to the following equation:

$$A = V_p/V_T - 100\%$$

where V_p is volume of pores; V_t is total volume of membrane.

2.4 Scanning electron microscopy (SEM)

SEM (Leo 1525 field emission scanning electron microscope, FESEM) was used to obtain images of cross-sectional areas of the tested membranes. After removing the backing material, membranes were snapped in liquid nitrogen, mounted onto SEM stubs, and coated with chromium using a chromium sputter coater (Emitech K575X). Applied SEM conditions were: a 7 mm working distance, and an inlens detector with an excitation voltage of 5 kV.

Nanofiltration experiments and hydrophilicity evaluation All nanofiltration experiments were carried out in a METcell cross-flow system, at 30° & 105 Pa with DMF or ethanol (EtOH) as a solvent and at 20°C. Permeate samples for flux measurements were collected at intervals of 1 h, and samples for rejection evaluation were taken after steady permeate flux was achieved. MWCO curves were obtained by using a standard test solution composed of a homologous series of styrene oligomers dissolved in DMF (EtOH was used only for measurement of pure solvent

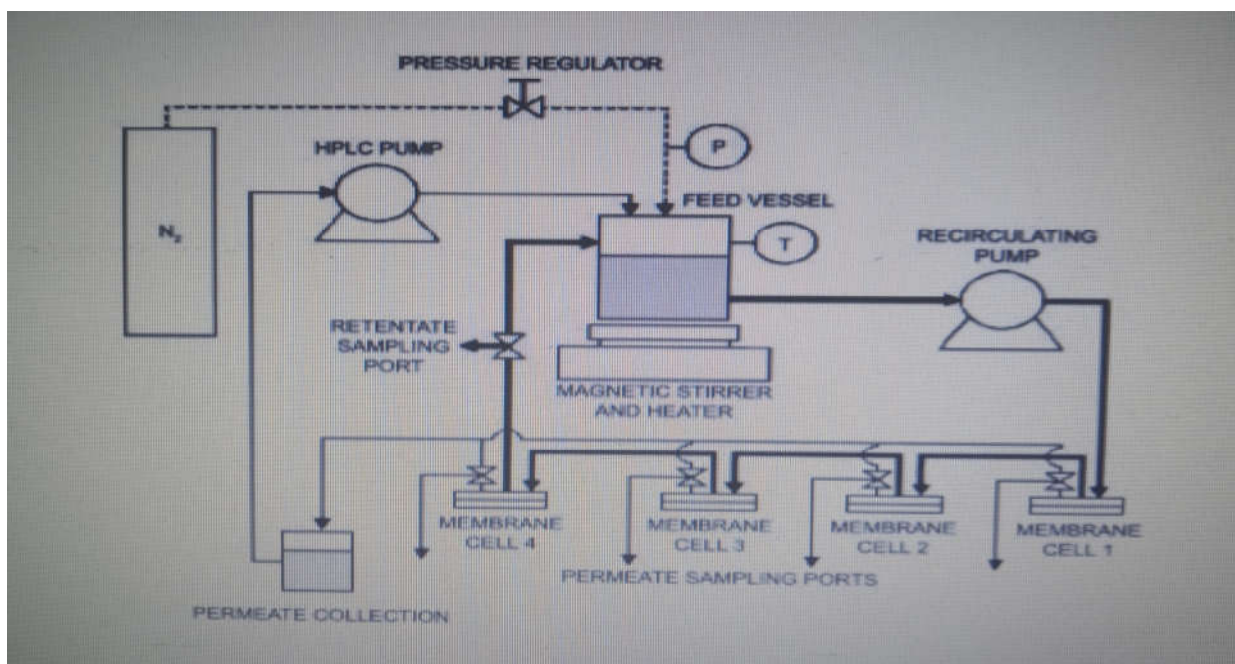
flux for the hydrophilicity comparison test). The styrene oligomer mixture contained 1 g L⁻¹ each of PS 580 and PS 1050 (Polymer Labs, UK), and 0.01 g L⁻¹ of 1-methylstyrene dimer (Sigma-Aldrich, UK). Concentrations of styrene oligomers in permeate samples were analysed using an Agilent HPLC system with a UV/Vis detector set at a wavelength of 264 nm. Separation was accomplished using an ACE 5-C18-300 column (Advanced Chromatography Technologies, ACT, UK). A mobile phase comprising 35 vol % analytical grade water and 65 vol % tetrahydrofuran with 0.1 vol % trifluoroacetic acid was used. Solvent flux (J) was determined by measuring the volume of permeate (V) per unit area (A) per unit time (t) according to the following equation:

$$J = V/A_t$$

Flux decrease of the membranes (DF) was calculated according to the following equation:

$$D_f = (A_i - A_s)/A_i$$

where J_i is initial flux; J_s is flux at steady state (achieved when two flux measurements within a 1 hour interval showed the same value within $\pm 2 \text{ L m}^{-2} \text{ h}^{-1}$). Rejection (R_i) of styrene oligomers was evaluated by applying equation (3) in which CP,i and CF,i correspond to styrene oligomers concentration in permeate and in feed solution, respectively. The corresponding molecular weight cut off curves were obtained from a plot of the rejection of styrene oligomers versus their molecular weight.



METcell cross-flow testing apparatus.

2.5 TGA analysis

Thermogravimetric analysis scans (TGA Q500 V6.7 Build 203) were performed at a heating rate of 20°C per min-1 up to 800°C, with helium as the purge gas. The membranes for TGA analysis were prepared without the backing material.

2.6 Mechanical strength test

Tensile strength was measured using an Instron 4466, Instron Corporation, with 5 kN load and a deformation speed of 5 mm per min-1. Five membranes of each type were tested to calculate the average tensile strength. The membranes were prepared without the backing material.

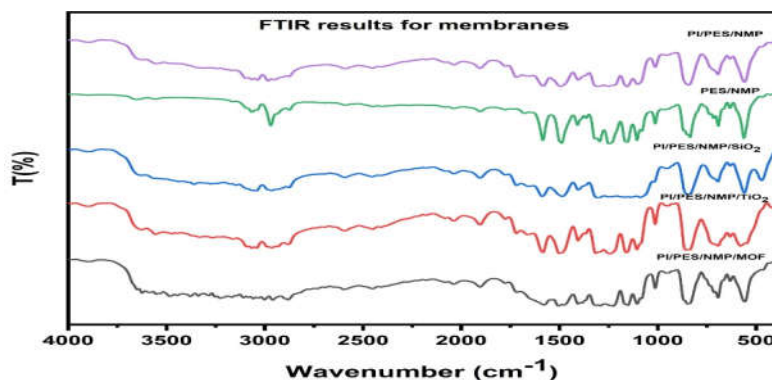
3 Results and discussion

3.1 Viscosity test

Viscosity of the dope solution is an important parameter. Increasing viscosity of dope solution is known to suppress macrovoid formation. The viscosity of dope solutions increases with higher TiO₂ loading. Higher rotational speed resulted in a viscosity decrease, and thus it can be concluded that PI/TiO₂ solutions behave as non Newtonian fluids. Depending on the TiO₂ concentration, rotational speed of the spindle of 0.5 RPM (3 and 5 wt. % TiO₂) or 0.6 RPM (0 and 1 wt.% TiO₂) corresponded to the lowest limit of shear rate and 3, 4, and 6 RPM corresponded the upper shear rate limit for 5, 3, and 1, 0 wt. % TiO₂, respectively.

3.2 FTIR analysis

The FTIR measurements were utilised to evaluate the efficiency of chemical crosslinking of the polymers under consideration. Figure shown below indicates that, when compared to non-crosslinked membranes, the signal intensity of imide bands at 1780, 1718, and 1351 cm increases for all four investigated polymers. Concurrently, the amipolymer-rich 1648 and 1534 cm⁻¹ were observed to rise, confirming the effective crosslinking events.

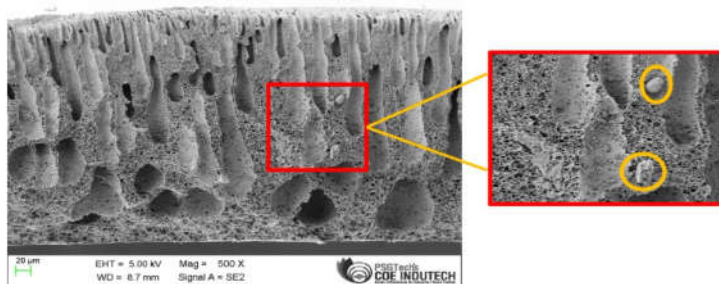
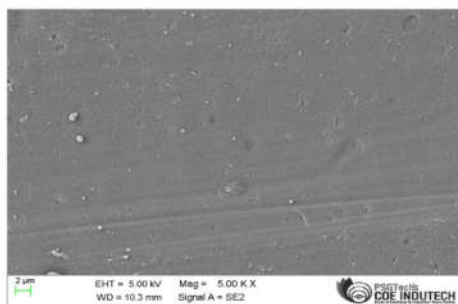


FTIR Analysis

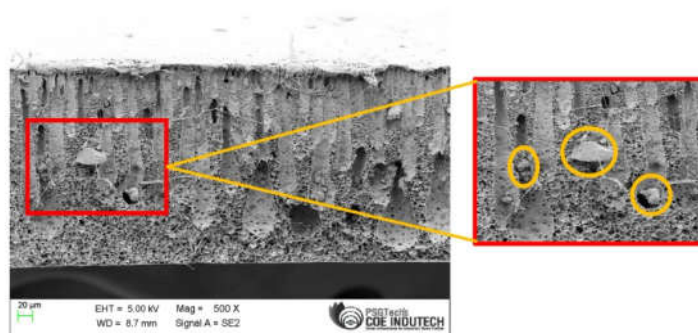
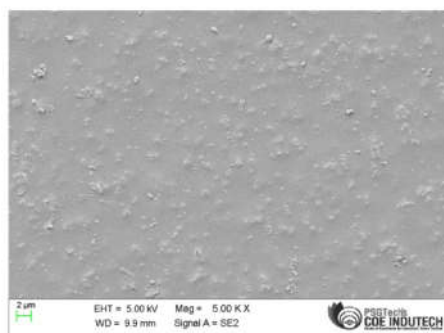
3.3 SEM ANALYSIS:

The analysis of Figures indicates that increasing 1,4-dioxane ratio depresses the macrovoid formation for the all four studied polyimides. This behaviour can be explained by the shift from instantaneous to delayed demixing, resulting from decreasing solvent/non-solvent affinity (increasing δ_S/δ_{NS}). Perhaps surprisingly, a comparison between the membrane matrix for different polyimides at all three studied DMF/1,4-dioxane ratio shows that the membranes prepared from P84 and HT are affected more by macrovoid formation. As stated earlier, the mutual solubility parameter NMP/NS is related to the size of the miscibility gap, and an increasing value implies that the size of the miscibility region decreases. MAT and UT have higher NMP/NS as compared to P84 and HT. Consequently, MAT and UT based membranes could be expected to be more affected by macrovoid formation. Nevertheless, one has to bear in mind that there are many factors affecting macrovoid formation, and the debate around this topic is still ongoing. Macrovoids grow from the nuclei of the polymer-lean phase. They can grow as long as no new nuclei are formed in their surroundings, and no polymer solidification takes place as this would freeze the void walls. One factor influencing macrovoid formation is polymer dope solution viscosity. If higher viscosity is a macrovoid-suppressor, as suggested in some literature a macrovoid-free matrix for MAT could be explained. However, UT would be expected to be more affected by macrovoids as compared to, for instance, P84, which has higher viscosity for all DMF:1,4-dioxane ratios. Yet the results indicate that UT based membranes are actually much less prone to macrovoid formation as compared to P84, suggesting that the viscosity explanation is unconvincing. Another possible phenomena taking place in the MAT and UT system is a quick solidification process. This means that once the binodal is crossed, the structure formed freezes quickly, there is not enough time for growth of macrovoids, and a sponge-like matrix is formed.

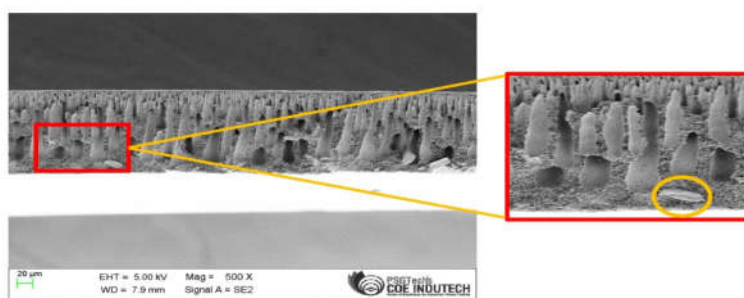
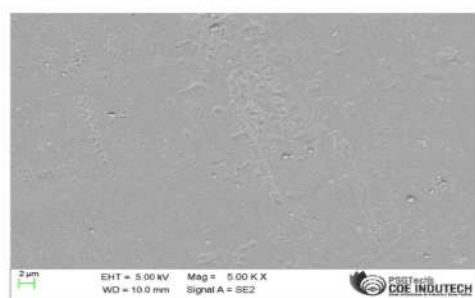
PI/PES/NMP/TiO₂



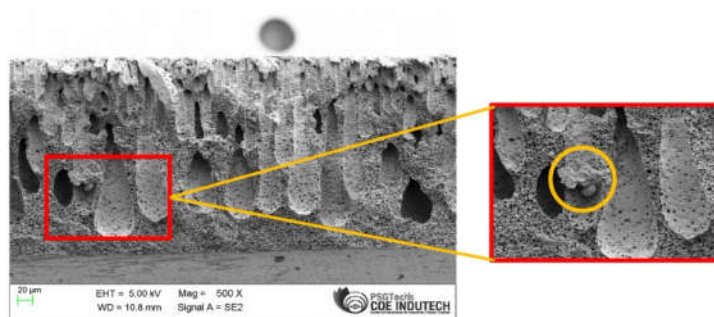
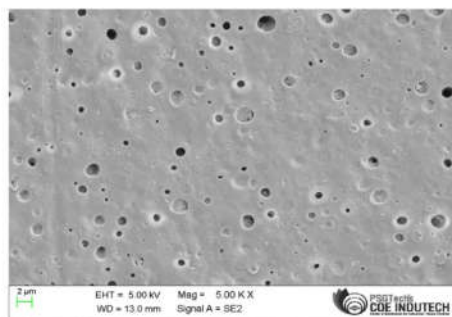
PI/PES/NMP/SiO₂



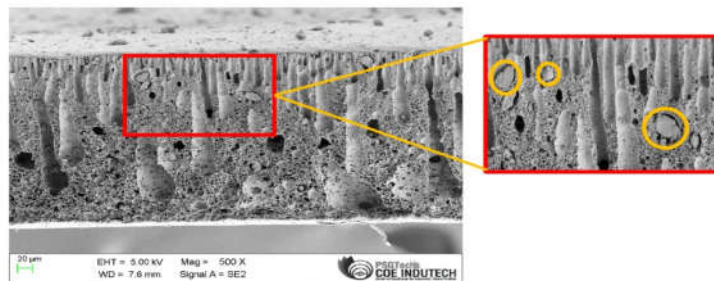
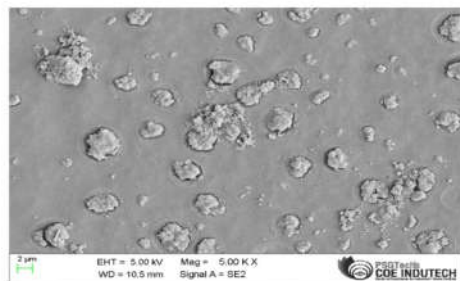
PES/NMP



PI/PES/NMP



PI/PES/NMP/MOF



SEM Analysis

4. CONCLUSION:

OSN membranes are a promising new type of liquid filtration membranes with a wide range of applications, including concentration, purification, and solvent exchange processes in organic media. The most recent generation of OSN membranes are solvent stable and can survive difficult operating conditions such as high temperatures and excessive pH. It has been shown that membrane processes offer a much higher productivity-to-volume ratio with larger scale. We have summarised current advances in OSN membranes from the standpoints of membrane materials and production methods. Above summarizes the state-of-the-art membrane performance in terms of permeance and rejection using ethanol, Methanol, and n-hexane feed solutions Furthermore, due to their strong coordination with the polymers, these nanofillers may alter the membrane surface attributes (such as roughness, hydrophilicity, zeta potential, and cross-linking degree), hence improving membrane permselectivity. As a result, efforts to leverage the specific features of nanomaterials like MOFs, and MOs in the selective layer of the membranes will continue to be a focus of research in OSN membrane development for the nanocomposite membranes to perform to their full potential. Membrane performance was proven to be influenced both by the characteristics of the nanoscale membrane morphology (expressed in the pore size and porosity) as well as by the molecular-level characteristics of the membrane polymer material. The choice of polymer and solvent system has been proven to strongly influence PI OSN membrane performance. The effect of polymer and solvent can be qualitatively predicted by the introduction of the complex solubility parameter

References:

- [1] Amirilargani, M., M. Sadrzadeh, E. J. R. Sudhölter, and L. C. P. M. De Smet. "Surface modification methods of organic solvent nanofiltration membranes." *Chemical Engineering Journal* 289 (2016): 562-582.
- [2] Joshi, Dirgha Raj, and Nisha Adhikari. "An overview on common organic solvents and their toxicity." *J. Pharm. Res. Int* 28, no. 3 (2019): 1-18.
- [3] Farahani, Mohammad Hossein Davood Abadi, and Vahid Vatanpour. "A comprehensive study on the performance and antifouling enhancement of the PVDF mixed matrix membranes

by embedding different nano particulates: clay, functionalized carbon nanotube, SiO₂, and TiO₂." *Separation and Purification Technology* 197 (2018): 372-381.

[4] Dai, Juan, Saisai Li, Jing Liu, Jing He, Jiding Li, Luying Wang, and Jiandu Lei. "Fabrication and characterization of a defect-free mixed matrix membrane by facile mixing PPSU with ZIF-8 core-shell microspheres for solvent-resistant nanofiltration." *Journal of Membrane Science* 589 (2019): 117261.

[5] Li, Can, Shuxuan Li, Long Tian, Jinmiao Zhang, Baowei Su, and Michael Z. Hu. "Covalent organic frameworks (COFs)-incorporated thin film nanocomposite (TFN) membranes for high-flux organic solvent nanofiltration (OSN)." *Journal of Membrane Science* 572 (2019): 520-531.

[6] Campbell, James, Joao Da Silva Burgal, Gyorgy Szekely, R. P. Davies, D. Christopher Braddock, and Andrew Livingston. "Hybrid polymer/MOF membranes for Organic Solvent Nanofiltration (OSN): Chemical modification and the quest for perfection." *Journal of Membrane Science* 503 (2016): 166-176.

[7] Chen, Xueming, Guohua Chen, and Po Lock Yue. "Separation of pollutants from restaurant wastewater by electrocoagulation." *Separation and purification technology* 19, no. 1-2 (2000): 65-76.

[8] Huang, Hua-Jiang, Shri Ramaswamy, U. W. Tschirner, and B. V. Ramarao. "A review of separation technologies in current and future biorefineries." *Separation and purification technology* 62, no. 1 (2008): 1-21.

[9] Komesu, Andrea, Maria Regina Wolf Maciel, and Rubens Maciel Filho. "Separation and purification technologies for lactic acid—A brief review." *BioResources* 12, no. 3 (2017): 6885-6901.